RESEARCH ARTICLE

Enhanced formation of trihalomethane disinfection byproducts from halobenzoquinones under combined UV/chlorine conditions

He Zhao[1,2], Ching-Hua Huang (✉)[2], Chen Zhong[1], Penghui Du[1,3], Peizhe Sun[2,4]

1 Beijing Engineering Research Center of Process Pollution Control, Division of Environment Technology and Engineering, Institute of Process Engineering, Chinese Academy of Sciences, Beijing 100190, China
2 School of Civil and Environmental Engineering, Georgia Institute of Technology, Atlanta, GA 30332, USA
3 State Environmental Protection Key Laboratory of Integrated Surface Water-Groundwater Pollution Control, School of Environmental Science and Engineering, Southern University of Science and Technology, Shenzhen 518055, China
4 School of Environmental Science and Engineering, Tianjin University, Tianjin 300072, China

HIGHLIGHTS

- 2,6-DCBQ and TCBQ generated THMs differently in chlorine and UV/chlorine processes.
- UV significantly enhanced hydroxylation of 2,6-DCBQ and CHCl$_3$ formation.
- THMs formation of DCBQ was enhanced due to UV benefitting excited DCBQ* hydrolysis.
- Hydroxylation and UV were both important for TCBQ in promoting THMs formation.
- High pH promoted hydroxylation of HBQs and CHCl$_3$ formation, especially for TCBQ.

GRAPHIC ABSTRACT
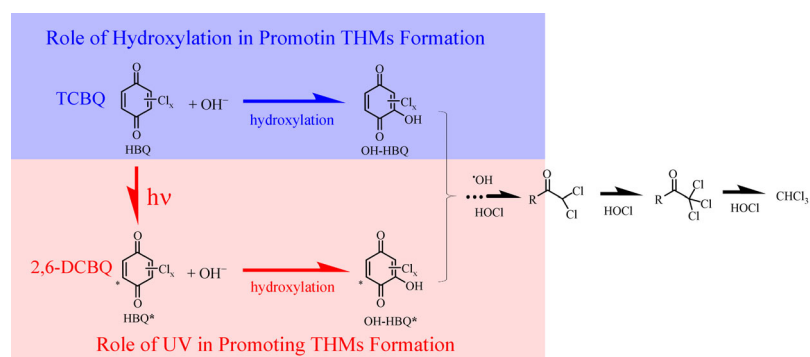
ARTICLE INFO

ABSTRACT

Halobenzoquinones (HBQs) are highly toxic disinfection byproducts (DBPs) and are also precursors of other DBPs such as trihalomethanes (THMs). The formation of THMs from HBQs during chlorine-only and UV/chlorine processes with or without bromide was investigated experimentally. Density functional theory (DFT) reactivity descriptors were also applied to predict the nucleophilic/electrophilic reactive sites on HBQs and intermediates. The results were combined to explain the different behaviors of 2,6-dichloro-1,4-benzoquinone (2,6-DCBQ) and tetrachloro-1,4-benzoquinone (TCBQ) and to propose mechanism for the promoting roles of UV and hydroxylation of HBQs in THMs formation. Under UV/chlorine, UV significantly enhanced THMs formation from 2,6-DCBQ compared to chlorine-only, mainly due to the production of OH-DCBQ*. Excited 2,6-DCBQ* by UV benefited nucleophilic hydrolysis to produce OH-DCBQ*, which favored electrophilic attack by chlorine, thereby inducing more THMs formation. UV/chlorine modestly promoted THMs formation from TCBQ compared to chlorine-only. Hydroxylation of TCBQ and UV irradiation were both important in promoting THMs formation due to the high electrophilic property of OH-TCBQ and TCBQ*. Meanwhile, hydroxylation of HBQs and CHCl$_3$ formation were enhanced at higher pH. This work suggested that enhanced formation of THMs from HBQs should be considered in the application of combined UV and chlorine processes.

1 Introduction

Halobenzoquinones (HBQs) are a group of compounds

✉ Corresponding author
E-mail: ching-hua.huang@ce.gatech.edu

identified as emerging disinfection by-product (DBP) due to their high toxicity (Li et al., 2015). The quantitative structure-toxicity relationship (QSTR) analysis predicts that HBQs are up to 1000 times more toxic than currently regulated DBPs, such as trihalomethanes (THMs) and haloacetic acids (HAAs) (Bull et al., 2006; Wu et al., 2020;

Wang et al., 2021). Recent studies have reported the presence of HBQs in drinking waters and swimming pool waters (Qin et al., 2010; Zhao et al., 2010; Zhao et al., 2012; Huang et al., 2013; Wang et al., 2013a; Pan et al., 2015), including 2,6-dichloro-1,4-benzoquinone (2,6-DCBQ), 2,3,6-trichloro-1,4-benzoquinone (TriCBQ), 2,3-dibromo-5,6-dimethyl-1,4-benzoquinone (DMDBBQ), 2,6-dichloro-3-methyl-1,4-benzoquinone (DCMBQ), 2,6-dibromo-1,4-benzoquinone (2,6-DBBQ), 2,5-dibromo-1,4-benzoquinone (2,5-DBBQ), tetrabromo-1,4-benzoquinone (TetraB-1,4-BQ), and tetrabromo-1,2-benzoquinone (TetraB-1,2-BQ), with 2,6-DCBQ being the most frequently detected (Wang et al., 2016). The occurrence of HBQs in potable and recreational waters poses a risk to the public health and the environment.

Ultraviolet (UV) irradiation is an alternative disinfection technology for water treatment, effective for inactivation of *Cryptosporidia*, *Giardia*, bacteria and viruses (Craik et al., 2001; Yang et al., 2020; Zhu et al., 2021). Compared to conventional free chlorine disinfectant, UV is advantageous for lower tendency to form harmful DBPs (Westerhoff et al., 2004; Hansen et al., 2013; Li et al., 2016; Zhang et al., 2018). A combination process of chlorine and UV may enhance the disinfection efficacy of chlorination (Young et al., 2018) and lower the demand for applied chlorine dose in water treatment. It has been reported that UV disinfection followed by chlorination is applied at more than 28 drinking water treatment plants in the US (Dotson et al., 2012). Moreover, UV treatment has been increasingly applied to chlorinated swimming pool waters for chloramine reduction and as a secondary disinfection process. In the combined UV and chlorine process, organic matter and other constituents in water are exposed to residual chlorine and UV simultaneously (Zhao et al., 2011; Hansen et al., 2013). Due to the formation of radical species from the photolysis of free chlorine, the combined UV/chlorine has been regarded as an advanced oxidation process (AOP) (Fang et al., 2014; Shu et al., 2014; Guo et al., 2017).

When UV is applied during the chlorination process, the DBP formation may be quite different from that under chlorine alone or UV alone. Several studies have indicated that UV irradiation combined with chlorination could promote the formation of DBPs. For example, Zhao et al. found enhanced formation of total organic halogen when nitrobenzene or benzoic acid was exposed to medium-pressure UV and chlorine simultaneously (Zhao et al., 2011). The combined process of low-pressure UV and chlorine was shown to significantly increase trichloronitromethane formation from amine precursors (Deng et al., 2014) and chloroform formation from phenolic precursors (Ben et al., 2016; Sharma et al., 2019)). Other studies also investigated how the combined UV and chlorination may affect the production of different reactive species (Fang et al., 2014; Guo et al., 2017; Gao et al., 2020) and therefore the degradation pathways of micro-pollutants in such systems (Ben et al., 2016; Mansor and Tay, 2020; Li et al., 2021).

Due to the high toxicity of HBQs, the environmental fate and transformation of HBQs have garnered many interests. Chlorination and chloramination of humic or anthropogenic phenolics (Wang et al., 2013b) constitute an important source of HBQs in water. HBQs are of transient nature – they are not only toxic chlorination intermediates but also precursors to form other DBPs such as THMs, tricholoroacetaldehyde and haloacetic acids (HAAs) depending on reaction conditions. Wang et al. (Wang et al., 2014) reported that HBQs could undergo oxidative transformation (induced by chlorine or alkaline conditions) and convert to halo-hydroxyl-benzoquinones (OH-HBQs) in drinking water treatment plants and distribution systems. Other studies (Qian et al., 2013; Richardson and Ternes, 2014) indicated that UV could also induce the transformation of HBQs into hydroxylated products. Thus, UV irradiation and high pH condition can both accelerate hydroxylation of HBQs. Due to structural similarity to chlorination intermediates of phenolic compounds (Chuang et al., 2015; Ben et al., 2016), HBQs and OH-HBQs may lead to DBPs such as THMs during chlorination. However, the formation of THMs from HBQs during chlorination or combined UV/chlorine processes had not been investigated systematically. Furthermore, it was unclear how UV and high pH condition might affect the reaction pathways of THMs formation from HBQs. Particularly, whether OH-HBQs may further affect the formation of THMs from HBQs during chlorination and UV/chlorine combined process needs further investigation.

In this study, we hypothesized that both hydroxylation and UV could promote the formation of THMs from HBQs. To test this hypothesis, the THMs formation from HBQs during the chlorination and combined UV/chlorine processes was investigated. A series of experiments were conducted to examine the effects of UV and pH on the THMs formation from HBQs, including the conditions with the presence of bromide. The roles of UV irradiation and hydroxylation of HBQs in enhancing THMs formation in the UV/chlorine process were specifically explored. Theoretical calculations were also applied to predict the nucleophilic/electrophilic reactivity and reactive sites of HBQs and intermediates to facilitate the understanding of reaction pathways. On the basis of the experimental and calculation results, the mechanism responsible for the enhancement effects of UV and hydroxylation of HBQs for THMs formation was proposed.

2   Materials and methods

2.1   Chemical and reagents

2-Chloro-1,4-benzoquinone (CBQ, 95%), 2,6-DCBQ

(98%), 2,5-dichloro-1,4-benzoquinone (2,5-DCBQ, 98%), tetrachloro-1,4-benzoquinone (TCBQ, 99%), chloroform (CHCl$_3$, 99.9%), bromodichloromethane (CHBrCl$_2$, $\geqslant$ 98%), dibromochloromethane (CHBr$_2$Cl, 98%), and bromoform (CHBr$_3$, 99%) were purchased from Sigma-Aldrich (St. Louis, MO). Sodium hypochlorite (NaOCl) solution containing about 5% free chlorine was purchased from Acros Organics (Fair Lawn, NJ). Hexane, methanol and ethanol of Optima LC/MS grade were obtained from Fisher Scientific (Fair Lawn, NJ). All other reagents used were obtained from Fisher Scientific and were of analytical grade. Deionized (DI) water (resistivity > 18.2 m$\Omega\cdot$cm) was generated by a Milli-Q Advantage A10 Ultrapure Water Purification System (Milllipore, Billerica, MA). The stock solutions of HBQs (10 mM, 0.1%FA) were prepared in methanol and stored at $-20°C$. The standards were diluted by DI water before use.

2.2 Experimental setup

Similar to our previous studies (Deng et al., 2014; Ben et al., 2016), all experiments were performed in a photochamber equipped with a magnetically stirred 100-mL cylindrical quartz reactor and a 4-W low-pressure UV lamp (G4T5 Hg lamp, Philips TUV4W). The quartz reactor was filled with 80 mL of HBQ solution (20 μM initial concentration) buffered by 0.2 M phosphate buffer to the desired pH value (pH 4.0–8.0). Sodium hypochlorite (initial free chlorine of 100 μM) was added into the quartz reactor to start the reaction. For the investigation of bromide effect, sodium bromide was added to samples (100 μM, [NaOCl]$_0$/[NaBr]$_0$ = 1.0) before the reaction. UV irradiation was supplied in the combined UV/chlorine or the UV-only experiments. The UV lamp was allowed to warm up for 30 min before the experiments. The UV fluence rate was determined to be around 2.12 $\times$ 10^{-6} Einstein/(L·s) using potassium ferrioxalate actinometry (Cai et al., 2017) and a UVX radiometer, equivalent to approximately 0.127 mW/cm^2 under the experimental setup. For experiments with UV, the reactor was placed inside the photochamber immediately after the chlorine addition. To monitor the reaction progress, sample aliquots were collected from the reactor and excess sodium thiosulfate was added immediately to quench the residual chlorine, followed by addition of 0.25% (v/v) formic acid to stabilize HBQs and OH-HBQs in the samples before analysis. Additionally, unquenched sample aliquots were collected and analyzed for residual chlorine in preliminary experiments using the N,N-diethyl-p-phenylenediamine (DPD) titrimetric method (Yang et al., 2018) and the results showed measurable free chlorine residuals at the end of the reaction time for most of the experimental conditions. For examining the possible influence of •OH radicals, 10 mM tert-butyl alcohol (TBA) or ethanol (EtOH) was added in the samples before the addition of free chlorine.

2.3 Analytical methods

Four THMs (CHCl$_3$, CHBrCl$_2$, CHBr$_2$Cl and CHBr$_3$) were measured following the US EPA method 551 with small modifications. Quantitative analysis was conducted using a gas chromatograph (6890, Agilent) with an electron capture detector and a HP-5MS capillary column (30 m $\times$ 0.25 mm, 0.25 μm). THMs were extracted from the water samples with hexane (recovery in the range of 95%–104%). Conditions for the GC analysis were as follows: injector temperature 200°C, column temperature from 35°C (held for 4 min) to 120°C (15°C/min then held for 2 min), and detector temperature 250°C. Calibration standards of THMs (0.01–50 μg/L) yielded a strong linear correlation (R^2 = 0.9992). The detection limit for THMs was around 0.1 μg/L. All experiments were conducted in triplicate or more.

HBQs and hydroxylated products were determined by a liquid chromatography/mass spectrometry system (Agilent 1100 HPLC/G1956B MSD) equipped with a Luna C18 column (100 mm $\times$ 2.0 mm, 3 μm; Phenomenex, Torrance, CA) at room temperature. The mobile phase consisted of solvent A (0.25% formic acid in water) and solvent B (0.25% formic acid in methanol) with a flow rate of 0.17 mL/min. A gradient program was performed as follows: linearly increased B from 20% to 90% in 20 min; kept B at 90% for 5 min; changed B to 20% for column re-equilibration at 25.1–40 min. The sample injection volume was 20 μL.

2.4 Computational methods

The density functional theory (DFT) and time-dependent density functional theory (TDDFT) were used to calculate the ground state and excited state of HBQs and OH-HBQs. The calculations were performed using the Gaussian 03 package (Smith, 2017). All geometries were fully optimized at the B3LYP/6-31G(d,p) level. Solvent effects were included by performing sing-point energy calculations on gas-phase optimized geometries with the SMD model in water at the B3LYP/6-31G(d,p) level of theory. DFT reactivity descriptors, including the global nucleophilicity/electrophilicity index (N and ω), the local nucleophilicity/electrophilicity index (N$_k$ and ω$_k$) and the condensed Fukui function index (f), were calculated to predict the reactivity and regioselectivity of HBQs and intermediates using Multiwfn software (Lu and Chen, 2012). Detailed calculation methods are presented in Supplementary Information (SI) Text S1 and Tables S1–S8.

3 Results

The potential of four HBQs, namely CBQ, 2,5-DCBQ, 2,6-DCBQ and TCBQ, to form THMs during chlorine and UV/

chlorine processes was evaluated and compared. Chloroform was the predominant THM formed in the UV/chlorine process (Fig. 1). Residual chlorine was measured at the end of each experiment, and confirmed that chlorine was not depleted during the reaction time course. For example, the residual free chlorine concentrations were 1.48 mg/L and 1.18 mg/L respectively after chlorine and UV/chlorine processes for 15 min (with $[NaOCl]_0 = 100$ μM (i.e., 7.1 mg/L)). To investigate the role of radicals in the UV/chlorine system, TBA, a hydroxyl radical (•OH) and chlorine radical (•Cl) scavenger, was added in some experiments with results shown in Figs. 1(c) and1(d). Addition of TBA increased the chloroform formation by 95.2% and 16.0% from 2,6-DCBQ and TCBQ, respectively, at the end of 15 min.

Moreover, the influence of pH on chloroform formation from 2,6-DCBQ and TCBQ during chlorine and UV/chlorine processes was examined as shown in Fig. 2. Previous studies reported that HBQs underwent spontaneous hydrolysis in neutral or weakly alkaline pH

conditions (Wang et al., 2014). The possible hydroxylated products of 2,6-DCBQ and TCBQ included mono-, di- and trichloro HBQs as presented in Fig. S1.

To explore the role of hydroxylation of HBQs in THMs formation, the effects of pH and UV irradiation on the generation of OH-HBQ products were studied (Figs. 3 and S2). Only the production of OH-DCBQ from 2,6-DCBQ and OH-TCBQ from TCBQ was compared because they were the major products. Due to the unavailability of authentic standards, the formation of OH-HBQs was quantified by the ratio of LC/MS peak area relative to that of the original HBQ.

When bromide was present in the solution during chlorine and UV/chlorine processes ($[NaOCl]_0/[NaBr]_0 = 1.0$), the formation of four THMs (including $CHCl_3$, $CHBrCl_2$, $CHBr_2Cl$ and $CHBr_3$) from 2,6-DCBQ and TCBQ was detected as shown in Figs. 4 and 5. EtOH, an efficient scavenger of hydroxyl radical and bromine (•Br) radical (Zhang and Parker, 2018), was added in the UV/chlorine system to assess the role of reactive species.
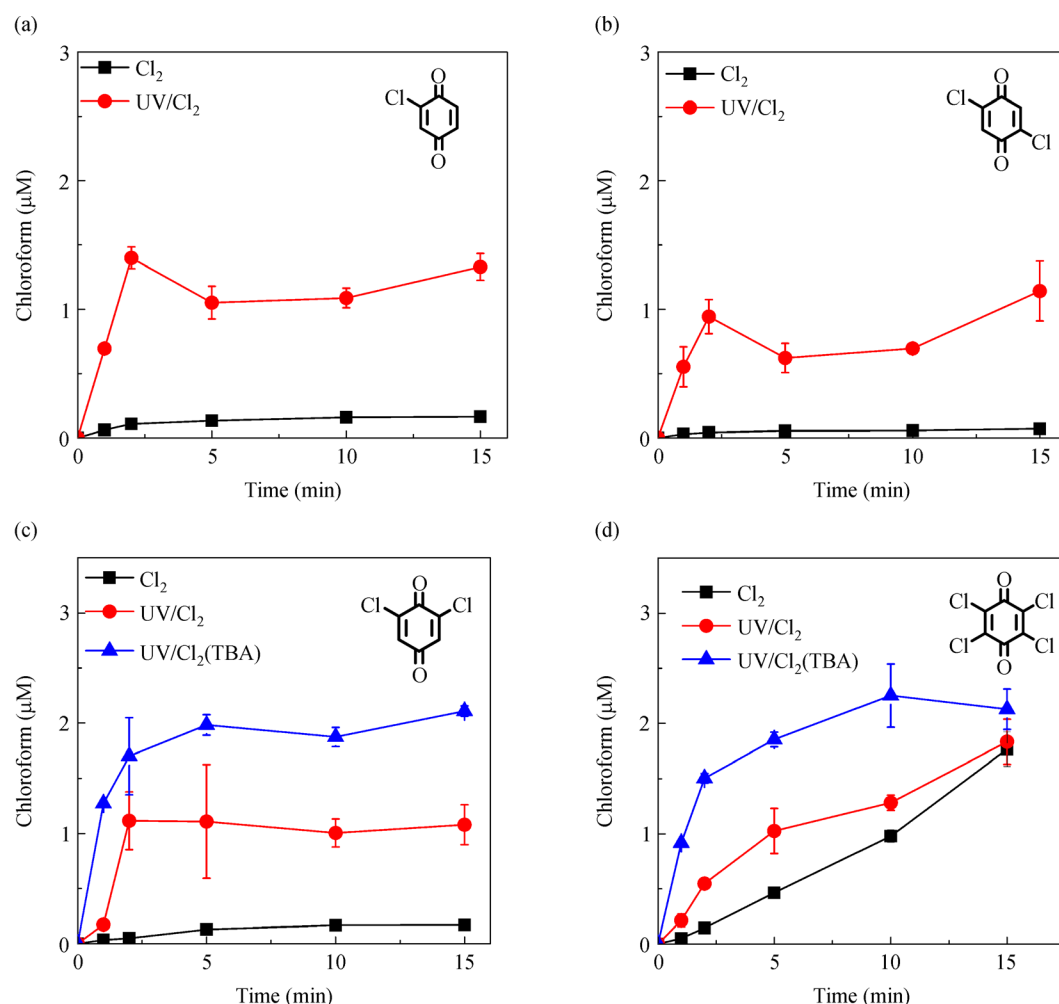

Fig. 1 Formation of chloroform from (a) CBQ, (b) 2,5-DCBQ, (c) 2,6-DCBQ and (d) TCBQ as a function of time by chlorine and UV/chlorine processes, including (c) 2,6-DCBQ, (d) TCBQ with the presence of TBA in the UV/chlorine process. ($[HBQs]_0 = 20$ μM, $[HClO]_0 = 100$ μM, pH = 7.0, UV = 3.9×10^{-6} Einstein/(L·s)).
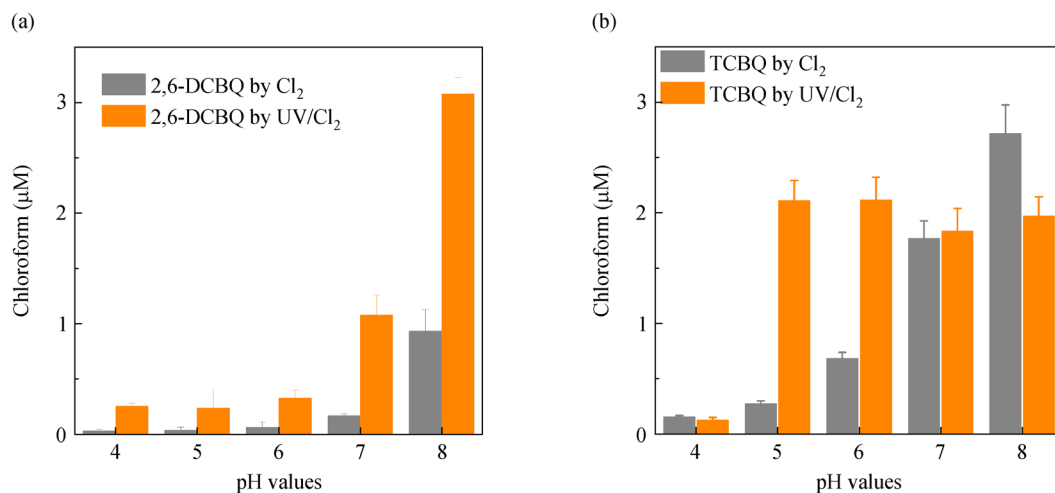
Fig. 2 Formation of chloroform from (a) 2,6-DCBQ and (b) TCBQ at different pHs by chlorine and UV/chlorine processes. ($[HBQ]_0 = 20$ μM, $[HClO]_0 = 100$ μM, reaction time = 15 min, UV = 3.9×10^{-6} Einstein/(L·s)).
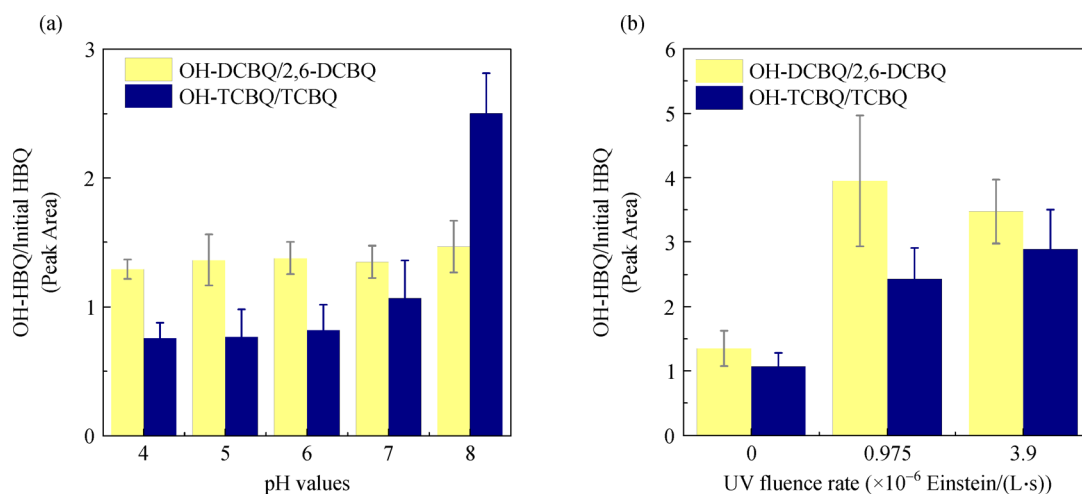

Fig. 3 Peak area ratios of the OH-HBQ products and the initial HBQ of 2,6-DCBQ and TCBQ: (a) effect of different pHs without UV irradiation, and (b) effect of UV irradiance at pH 7.0. ($[HBQ]_0 = 20$ μM, reaction time = 15 min).
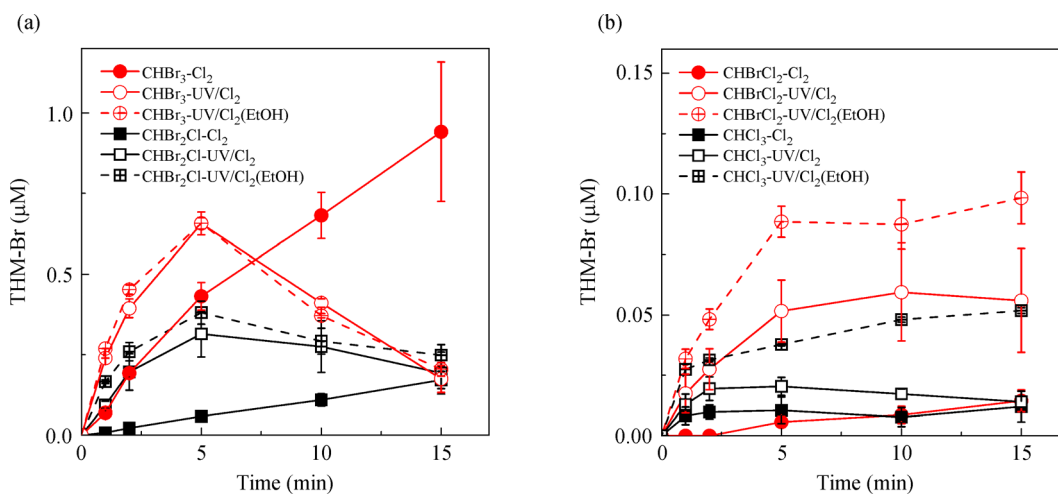

Fig. 4 Formation of (a) $CHBr_2Cl$ and $CHBr_3$, (b) $CHBrCl_2$ and $CHCl_3$ from 2,6-DCBQ with the presence of bromide by chlorine and UV/chlorine processes. ($[2,6\text{-}DCBQ]_0 = 20$ μM, $[HClO]_0 = 100$ μM, $[Br^-]_0 = 100$ μM, pH = 7.0, UV = 3.9×10^{-6} Einstein/(L·s)).
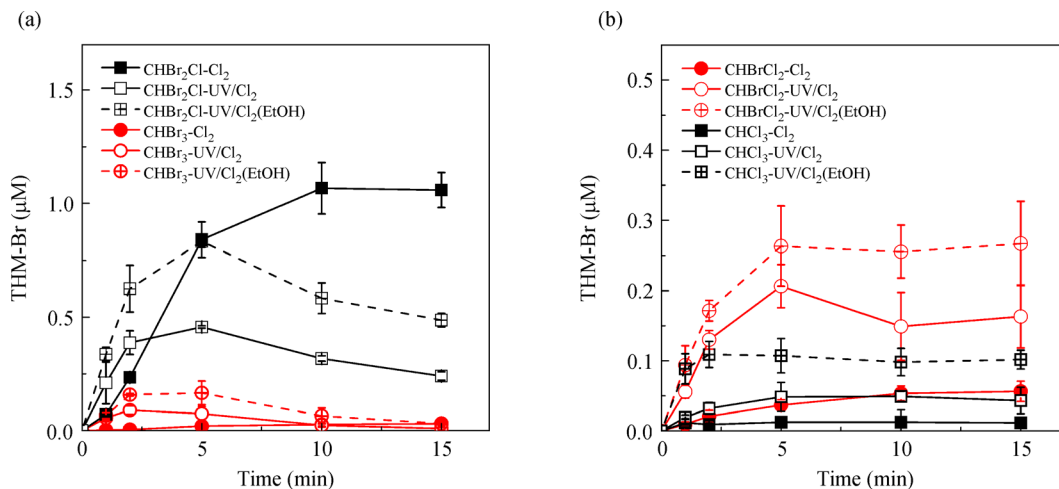
Fig. 5 Formation of (a) CHBr$_2$Cl and CHBr$_3$, (b) CHBrCl$_2$ and CHCl$_3$ from TCBQ with the presence of bromide by chlorine and UV/chlorine processes. ([TCBQs]$_0$ = 20 μM, [HClO]$_0$ = 100 μM, [Br$^-$]$_0$ = 100 μM, pH = 7.0, UV = 3.9 × 10^{-6} Einstein/(L·s)).

Figure 6 presents the effect of pH on the formation of CHBr$_3$, CHBr$_2$Cl, CHBrCl$_2$ and CHCl$_3$ from 2,6-DCBQ and TCBQ with the presence of bromide during chlorine and UV/chlorine processes.

The nucleophilic/electrophilic characteristics of HBQs and intermediates (i.e., OH-HBQs and excited HBQs) during hydrolysis and/or UV irradiation greatly affected the formation potential of THMs. To further explore the mechanism of HBQs and intermediates in the formation of THMs, the global nucleophilicity/electrophilicity index (N and ω, Table 1) of those were calculated based on density functional reactivity theory. For HBQs and intermediates in this study, those possess a higher value in the global nucleophilicity index (N, eV) were more easily attacked by chlorine electrophile, while those possess a higher value in the global electrophilicity index (ω, eV) more easily

undergo hydrolysis by nucleophilic attack of hydroxide ion. Then, the reactive sites of HBQs and intermediates were predicted as shown in Fig. 7 according to the local nucleophilicity index (N$_k$, e*eV) and local electrophilicity index (ω$_k$, e*eV). For HBQs and intermediates, the structure sites with the highest local nucleophilicity/ electrophilicity index indicated most reactive for chlorine oxidation or hydroxyl hydrolysis, respectively. Some details in the DFT calculations are shown in SI and Tables S1−S8.

4 Discussion

According to the above results, we found that both hydroxylation and UV can promote THMs formation
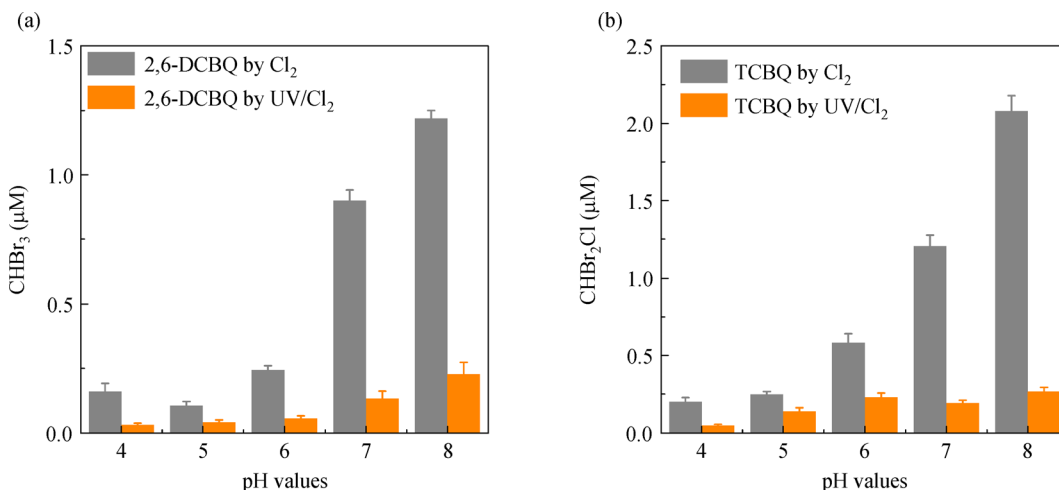

Fig. 6 The (a) formation of CHBr$_3$ from 2,6-DCBQ, and (b) formation of CHBr$_2$Cl from TCBQ with the presence of bromide by chlorine and UV/chlorine processes at different pHs. ([HBQ]$_0$ = 20 μM, [HClO]$_0$ = 100 μM, [Br$^-$]$_0$ = 100 μM, reaction time = 15 min, UV = 3.9 × 10^{-6} Einstein/(L·s)).

Table 1 The global nucleophilicity index and global electrophilicity index of HBQs and intermediates

HBQs	Global nucleophilicity index (N, eV)	Global electrophilicity index (ω, eV)
2,6-DCBQ	1.4136	2.2299
OH-DCBQ	1.9794	1.9838
2,6-DCBQ*	1.1431	2.6376
OH-DCBQ*	2.3853	2.6548
TCBQ	1.6415	2.4543
OH-TCBQ	2.2708	2.2616
TCBQ*	1.3711	2.4963
OH-TCBQ*	1.8629	2.3401
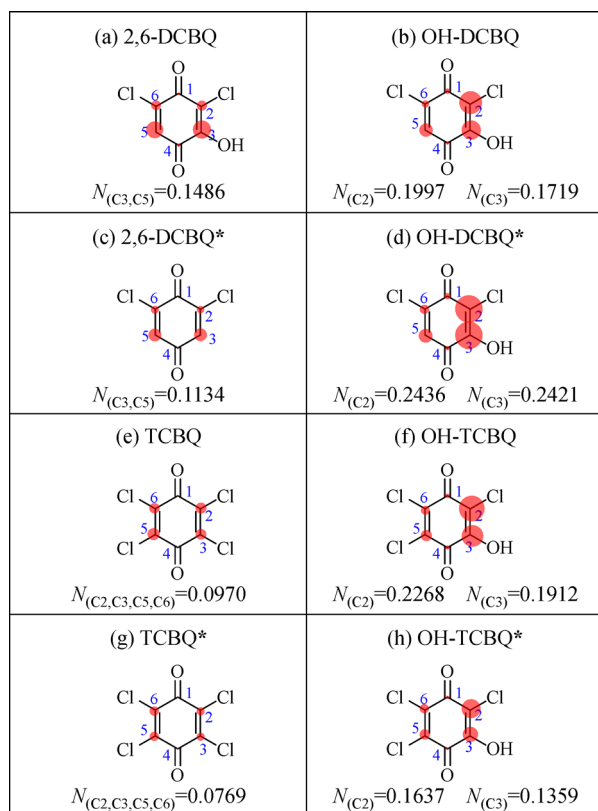
Fig. 7 Prediction of chlorination reactive sites on HBQs and intermediates by the local nucleophilicity index (N_k, e*eV) calculation (The N_k index is visualized by the diameter of red circles, a bigger red circle indicating a higher N_k index). (a) 2,6-DCBQ, (b) OH-DCBQ, (c) 2,6-DCBQ*, (d) OH-DCBQ*, (e) TCBQ, (f) OH-TCBQ, (g) TCBQ* and (h) OH-TCBQ*.

from HBQs in chlorination. The promoting roles of hydroxylation and UV are discussed in detail as follows.

4.1 THMs formation from HBQs during chlorination

During chlorination, the chloroform formation from CBQ, 2,5-DCBQ, 2,6-DCBQ and TCBQ, respectively, increased

with reaction time (Fig. 1). The yield of $CHCl_3$ formation from HBQs showed the trend of TCBQ $\gg$ 2,6-DCBQ $\approx$ 2,5-DCBQ $\approx$ CBQ. Furthermore, the chloroform formation from 2,6-DCBQ and TCBQ under chlorination can be significantly promoted by an increase in pH, especially for TCBQ (Fig. 2). The strong pH influence is probably related to the fact that HBQs undergo spontaneous hydrolysis in a neutral or weakly basic pH environment (Wang et al., 2014), even though a higher pH decreased the concentration of HOCl species, a stronger oxidant than the OCl^- species (Dodd and Huang, 2004). Higher pH values often lead to an enhanced THMs formation initiated by hydrolysis (Mellahi et al., 2015). The production of OH-DCBQ or OH-TriCBQ from 2,6-DCBQ or TCBQ via hydrolysis was observed to increase with time at pH 8.0 (Fig. S2(a)). Higher pH values enhanced the hydroxylation of 2,6-DCBQ and TCBQ, and this effect was considerably stronger for TCBQ than for 2,6-DCBQ (Fig. 3(a)). The greater hydroxylation rate at a higher pH is because OH^- is much more reactive than H_2O to bind with HBQs due to the high electron density around oxygen atom (Wang et al., 2014). At pH 8.0, the concentrations of OH^- was around 1 μM with the presence of PBS, which was approximate to the concentration of HBQs, and would significantly increase the hydrolysis of TCBQ.

DFT analysis further verified that hydrolysis could significantly affect the reactive characteristics of HBQs for chlorine oxidation (Table 1). First, the global nucleophilicity index (N) followed the trend of $N_{OH-HBQs} > N_{HBQs}$, suggesting that hydrolyzed HBQs were more favorable for chlorine attack. Due to the increased nucleophilic reactivity of OH-HBQs, hydroxylation played an important role in promoting THMs formation from HBQs during chorination. This was similar to the enhanced coupling of intermediates during the further oxidation steps reported previously (Zhong et al., 2020). Figure 7 illustrated that the highest local nucleophilicity index (N_k) of OH-DCBQ and OH-TCBQ occurred at C2, suggesting that it was the most favorable site for chlorination. Additionally, 2,6-DCBQ and TCBQ had different priorities for hydrolysis. The comparison of the global electrophilicity index between different HBQs was $\omega_{TCBQ} > \omega_{DCBQ}$ (Table 1). These results indicated that TCBQ was more favorable than DCBQ for hydroxylation. This conclusion was in accordance with the pH effect mentioned above, in that TCBQ could produce more OH-HBQ products at a higher pH value than 2,6-DCBQ. Furthermore, the highest global nucleophilicity index of OH-TCBQ indicated that OH-TCBQ was more favorable than 2,6-DCBQ and OH-DCBQ for chlorine oxidation. Thus, the THMs formation from TCBQ was greatly increased when pH was increased.

4.2 THMs formation from HBQs during chlorination with the presence of bromide

When bromide was present in the system ($[NaOCl]_0$/

[NaBr]$_0$ = 1.0), the THMs formation from 2,6-DCBQ and TCBQ gradually increased with time during the chlorine process (Figs. 4 and 5). The yields of THMs formation from 2,6-DCBQ showed the trend of CHBr$_3$ $\gg$ CHBr$_2$Cl $\gg$ CHBrCl$_2$ $\approx$ CHCl$_3$, and those from TCBQ showed the trend of CHBr$_2$Cl $\gg$ CHBr$_3$ $\approx$ CHBrCl$_2$ > CHCl$_3$. CHBr$_3$ contributed to the majority of THMs formation of 2,6-DCBQ, while CHBr$_2$Cl was the main THM formed from TCBQ. Figs. 4(a) and 5(a) also indicated that THMs formation from TCBQ was slightly higher and faster than that of 2,6-DCBQ.

Furthermore, pH had a significant effect on THMs formation from both 2,6-DCBQ and TCBQ during chlorination with the presence of bromide. As Figure 6 shows, CHBr$_3$ formation from 2,6-DCBQ and CHBr$_2$Cl formation from TCBQ both increased with increasing pH value during chlorination. This agreed with what was mentioned above that higher pH values enhanced the hydroxylation of 2,6-DCBQ and TCBQ. Interestingly, although TCBQ had a higher priority for hydrolysis than 2,6-DCBQ (Table 1), the pH effect was not stronger for TCBQ than for 2,6-DCBQ during chlorination with the presence of bromide. For the formation of brominated THMs (Br-THMs), there was no significant difference between DCBQ and TCBQ by pH effect, which probably was due to a higher oxidation ability of HOBr than HOCl (Westerhoff et al., 2004). Although a higher nucleophilic reactivity of OH-TCBQ than OH-DCBQ for chlorine (Du et al., 2017), oxidation ability plays a more important role in promoting THMs formation from HBQs during chorine process with the presence of bromide.

4.3   THMs formation from HBQs during UV/Chlorine

When UV was combined with chlorine, the formation of chloroform from CBQ, 2,5-DCBQ and 2,6-DCBQ was significantly promoted (Fig. 1), with the CHCl$_3$ yield increased by almost 10-times compared to that under chlorine alone (Figs. 1(a)−1(c)). On the other hand, UV only modestly promoted the CHCl$_3$ formation from TCBQ (Fig. 1(d)). Furthermore, when TBA was present in the UV/chlorine system, the CHCl$_3$ formation of 2,6-DCBQ and TCBQ increased almost 100% (Figs. 1(c) and 1(d)). The effect of TBA addition was to scavenge radicals, and the photolysis of TBA under UV/chlorine did not lead to THMs formation as indicated by other studies (Oliver and Carey, 1977; Ben et al., 2016). It is known that UV photons excite HOCl and OCl$^-$ to generate several radicals such as •OH and •Cl in the combined UV/chlorine process (Ben et al., 2016; Sharma et al., 2019). The radicals can hinder THMs formation and UV irradiation can degrade THMs with the kinetic constant ranging from 0.020 min^{-1} (chloroform) to 0.390 min^{-1} (bromoform) (Hansen et al., 2013). Meanwhile, absorption of UV light can induce HBQs into the excited state HBQs*, which can be oxidized and transformed into CHCl$_3$ by HOCl (Sharma et al., 2017;

Zhang et al., 2021). In this study, UV may enhance the formation of chloroform from HBQs*, but radicals can also destroy the structure of HBQs*. Thus, more CHCl$_3$ was generated when radicals were scavenged, implying the structure of HBQs* was more likely to yield chloroform than HBQs. It also suggested that absorption of UV and direct oxidation of HOCl might play an important role in the transformation of HBQs into chloroform in the combined UV/chlorine treatment.

In the UV/chlorine process, Fig. 2(a) shows the CHCl$_3$ yield of 2,6-DCBQ increased as pH was increased. Compared to the chlorine-only process, the chloroform formation of 2,6-DCBQ under UV/chlorine was significantly promoted by higher pH conditions, which implied a more important role of hydroxylation of 2,6-DCBQ in CHCl$_3$ yield, and possibly a greater role of OCl$^-$ species excitation by light (Sun et al., 2016). For TCBQ (Fig. 2(b)), in contrast, a higher pH value from 5.0 to 8.0 did not enhance the chloroform formation in UV/chlorine system. Actually, slightly higher CHCl$_3$ formation from TCBQ occurred at lower pH range (pH 5.0–6.0) than at the higher pH range (pH 7.0-8.0). Thus, hydroxylation of TCBQ was not important for CHCl$_3$ formation in UV/chlorine system, while TCBQ* may play a more important role.

The effect of UV irradiation on the OH-HBQ products was also studied in UV/chlorine system. As Fig. S2b shows, UV significantly increased OH-HBQs generation almost immediately, more so for 2,6-DCBQ than TCBQ, and then the OH-HBQs abundance decreased with time. Thus, OH-HBQs were not only the hydrolysis product of HBQs, but also were the precursors of THMs. The hydroxyl group of OH-HBQs is an electron-donating group, which can benefit chlorination process (Yang et al., 2018) and promote THMs formation. Furthermore, the effects of pH and UV showed differences between TCBQ and 2,6-DCBQ. On one hand, Cl as a leaving group may be more easily replaced by hydroxide (Smith, 2017). Thus, more TCBQ can be hydroxylated during chlorine process. On the other hand, UV could change electron distribution of 2,6-DCBQ and TCBQ. Newly formed HBQs* may behave considerably different in hydrolysis and as THMs formation precursors.

When HBQ was irradiated by UV, the excited HBQ* may show significantly different electrophilic/nucleophilic characteristics than the ground-state HBQ (Table 1 and Fig. 7). Table 1 showed 2,6-DCBQ* had a higher global electrophilicity index, benefiting nucleophilic hydrolysis and more OH-DCBQ* product. It was consistent with Fig. S2(b) data for instant increase of OH-DCBQ under UV irradiation. Due to the highest global nucleophilicity index, OH-DCBQ* was more susceptible for attack by chlorine. Thus, UV could significantly enhance THMs formation of 2,6-DCBQ during chlorine process. Fig. 7(d) also shows that the highest local nucleophilicity index of OH-DCBQ* occurred at C2 and C3 sites, indicating they

were the most favorable sites for chlorination.

For excited TCBQ*, it was highly symmetric that C2, C3, C5 and C6 were four equivalent sites (Fig. 7(g)) with high electron repulsion (Table 1). Therefore, TCBQ* could be more easily attacked by the electrophilic agent HOCl but not by the nucleophilic agent OH⁻. Thus, UV did not significantly increase OH-TCBQ formation. UV promoted TCBQ* formation appeared to be the main role in CHCl₃ formation. This was consistent with the pH effect and DFT analysis mentioned above. However, TCBQ* was not much better than OH-TCBQ for HOCl attack (Table 1). Thus, TCBQ* did not show a significant increase of CHCl₃ formation, which indicated a switch of CHCl₃ formation mechanism for TCBQ when UV was applied in the chlorine process.

The mechanism of promoting roles of UV and hydroxylation in THMs formation from HBQs under UV/chlorine can be proposed for 2,6-DCBQ and TCBQ, respectively, owing to their different behaviors. For 2,6-DCBQ, UV can significantly enhance THMs formation by forming 2,6-DCBQ* which is more susceptible to nucleophilic hydrolysis to produce OH-DCBQ*. The hydrolyzed product OH-DCBQ* favors electrophilic attack by HOCl, thereby inducing more THMs formation. For TCBQ, the hydroxylation of TCBQ and UV irradiation both play an important role in THMs formation. Among the HBQs, TCBQ is favorable for hydrolysis to produce OH-TCBQ, which can be easily attacked by electrophilic HOCl. TCBQ* formed by UV irradiation possesses enhanced electrophilic ability toward HOCl. Thus, both hydroxylation and UV enhanced THMs formation.

4.4 THMs formation from HBQs during UV/Chlorine with the presence of bromide

When bromide was present in the UV/chlorine system ([NaOCl]₀/[NaBr]₀ = 1.0), the THMs formation from HBQs is shown in Figs. 4 and 5. The yields of THMs formation followed the trend of CHBr₃ > CHBr₂Cl > CHBrCl₂ > CHCl₃ for 2,6-DCBQ, and the trend of CHBr₂Cl ≫ CHBr₃ ≈ CHBrCl₂ > CHCl₃ for TCBQ. CHBr₃ contributed to the majority of THMs formation of 2,6-DCBQ, while most of THMs formation from TCBQ was CHBr₂Cl. The dominance of specific THMs in the UV/chlorine with Br⁻ system was similar to that in the chlorine-only with bromide system. The DFT calculation results were also in agreement with the Br-THMs formation from HBQs in the chlorine-only or UV/chlorine with bromide systems. Because there was no chlorine substituent on the favorable reactive sites (C3 and C5) of 2,6-DCBQ and OH-DCBQ*, more CHBr₃ was produced via electrophilic attack by HOBr (Fig. 6) (Zhang et al., 2021). With chlorine substituent on the electrophilic sites (C2, C3, C5 and C6) of TCBQ and OH-TCBQ*, majority THMs formation of was CHBr₂Cl (Fig. 6).

When bromide was present in the system, the THMs formation from HBQs increased initially to reached a maximum at around 5 min and then decreased afterwards in the UV/chlorine system, which differed from the gradual increase of THMs formation with time during the chlorine-only process (Figs. 4 and 5). Before the THMs began to decrease, UV/chlorine with Br⁻ system led to an increase of CHBr₃ formation from 2,6-DCBQ (Fig. 4(a)) but a decrease of CHBr₂Cl formation from TCBQ (Fig. 5(a)) in comparison with the chlorine with Br⁻ system.

The formation of CHBr₃ and CHBr₂Cl was attributed to the oxidation of bromide ion to HOBr and OBr⁻ by chlorine (Zhang and Parker, 2018). Under UV irradiation, HOBr and OBr⁻ mainly decompose to yield •OH and •Br (Fang and Shang, 2012). Addition of EtOH, an efficient scavenger of hydroxyl and bromine radicals, minimally affected the CHBr₃ formation from 2,6-DCBQ (Fig. 4(a)), but decreased and then increased the CHBr₂Cl formation from TCBQ (Fig. 5(a)). The above results indicated that hydroxyl radicals and bromine radicals had little effect in the CHBr₃ formation of 2,6-DCBQ in the UV/chlorine with Br⁻ system. Additionally, hydroxyl radicals and bromine radicals can destroy the structure of TCBQ* excited by UV irradiation. The results that more CHBr₂Cl was generated when radicals were scavenged indicated that the structure of TCBQ* played an important role in Br-THMs formation. Thus, besides UV and HOBr oxidation, different structures of HBQs also affected the THMs formation from HBQs in the combined UV/chlorine treatment with the presence of bromine.

Moreover, UV could induce the decomposition of Br-THMs, especially for CHBr₃ (Fig. S3). This result is consistent with previous study indicating the bond dissociation energy of C-Br is lower than that of C-Cl (Saha et al., 2013). Thus, the THMs formation from HBQs decreased after several minutes in the UV/chlorine with Br⁻ system, due to decomposition of Br-THMs by UV irradiation. Fig. 6 also shows that the pH value had only moderate effect on the CHBr₃ and CHBr₂Cl formation from 2,6-DCBQ and TCBQ, respectively. Even so, the pH influence was likely similar to that in UV/chorine system, but due to significant decay of Br-THMs by UV, the importance of pH influence became less pronounced.

5 Conclusions

The results of this study have shed light on the following key conclusions:

1) 2,6-DCBQ and TCBQ, while both are HBQs, showed different behaviors for the THMs formation during chlorine and UV/chlorine processes.

2) UV could significantly enhance the hydroxylation of 2,6-DCBQ and CHCl₃ formation by almost 10 times. The main reason could be attributed to the production of OH-DCBQ*. Excited 2,6-DCBQ* by UV could benefit nucleophilic hydrolysis to produce OH-DCBQ*, which

favored electrophilic attack by chlorine, thereby inducing more THMs formation.

3) Hydroxylation of TCBQ and UV irradiation were both important in promoting THMs formation due to the high electrophilic ability of OH-TCBQ and TCBQ*. Furthermore, hydroxylation of TCBQ and higher CHCl$_3$ formation can be enhanced by a higher pH value.

In this study, while the experiments were monitored up to 15 min, the impact of UV in the UV/chlorine process occurred rapidly and prominently in the beginning of the reaction period. Thus, the findings of this study are also useful for much shorter UV exposure time. Prolonged UV exposure, on the other hand, could lead to some degradation of the formed THMs (particularly Br-THMs) at a later stage.

References

Ben W, Sun P, Huang C H (2016). Effects of combined UV and chlorine treatment on chloroform formation from triclosan. Chemosphere, 150: 715–722

Bull R J, Reckhow D A, Rotello V, Bull O M, Kim J (2006). Use of Toxicological and Chemical Models to Prioritize DBP Research. #2867., A.R.F.a.E.p. ed. Boston: Academic Press

Cai M, Sun P, Zhang L, Huang C H (2017). UV/Peracetic Acid for Degradation of Pharmaceuticals and Reactive Species Evaluation. Environmental Science & Technology, 51(24): 14217–14224

Chuang Y H, McCurry D L, Tung H H, Mitch W A (2015). Formation pathways and trade-offs between *Haloacetamides* and *Haloacetaldehydes* during combined chlorination and chloramination of lignin phenols and natural waters. Environmental Science & Technology, 49(24): 14432–14440

Craik S A, Weldon D, Finch G R, Bolton J R, Belosevic M (2001). Inactivation of *Cryptosporidium parvum* oocysts using medium- and low-pressure ultraviolet radiation. Water Research, 35(6): 1387–1398

Deng L, Huang C H, Wang Y L (2014). Effects of combined UV and chlorine treatment on the formation of trichloronitromethane from amine precursors. Environmental Science & Technology, 48(5): 2697–2705

Michael C. Dodd and Ching-Hua Huang (2004). Transformation of the Antibacterial Agent Sulfamethoxazole in Reactions with Chlorine: Kinetics, Mechanisms, and Pathways. Environmental Science & Technology, 38(21): 5607–5615

Dotson A D, Rodriguez C E, Linden K G (2012). UV disinfection implementation status in US water treatment plants. Journal AWWA, 104(5): E318–E324

Du P, Zhao H, Cao H, Huang C H, Liu W, Li Y (2017). Transformation

of halobenzoquinones with the presence of amino acids in water: Products, pathways and toxicity. Water Research, 122: 299–307

Fang J, Fu Y, Shang C (2014). The roles of reactive species in micropollutant degradation in the UV/free chlorine system. Environmental Science & Technology, 48(3): 1859–1868

Fang J Y, Shang C (2012). Bromate formation from bromide oxidation by the UV/persulfate process. Environmental Science & Technology, 46(16): 8976–8983

Gao Z C, Lin Y L, Xu B, Xia Y, Hu C Y, Zhang T Y, Qian H, Cao T C, Gao N Y (2020). Effect of bromide and iodide on halogenated by-product formation from different organic precursors during UV/chlorine processes. Water Research, 182:116035

Guo K, Wu Z, Shang C, Yao B, Hou S, Yang X, Song W, Fang J (2017). Radical chemistry and structural relationships of PPCP degradation by UV/Chlorine treatment in simulated drinking water. Environmental Science & Technology, 51(18): 10431–10439

Hansen K M S, Zortea R, Piketty A, Vega S R, Andersen H R (2013). Photolytic removal of DBPs by medium pressure UV in swimming pool water. Science of the Total Environment, 443: 850–856

Huang R, Wang W, Qian Y, Boyd J M, Zhao Y, Li X F (2013). Ultra pressure liquid chromatography-negative electrospray ionization mass spectrometry determination of twelve halobenzoquinones at ng/L levels in drinking water. Analytical Chemistry, 85(9): 4520–4529

Li J, Wang W, Moe B, Wang H, Li X F (2015). Chemical and toxicological characterization of halobenzoquinones, an emerging class of disinfection byproducts. Chemical Research in Toxicology, 28(3): 306–318

Li T, Jiang Y, An X, Liu H, Hu C, Qu J (2016). Transformation of humic acid and halogenated byproduct formation in UV-chlorine processes. Water Research, 102: 421–427

Li X, Li Z, Xing Z, Song Z, Ye B, Wang Z, Wu Q (2021). UV-LED/P25-based photocatalysis for effective degradation of isothiazolone biocide. Frontiers of Environmental Science & Engineering, 15(5): 85

Lu T, Chen F (2012). Multiwfn: A multifunctional wavefunction analyzer. Journal of Computational Chemistry, 33(5): 580–592

Mansor N A, Tay K S (2020). Potential toxic effects of chlorination and UV/chlorination in the treatment of hydrochlorothiazide in the water. Science of the Total Environment, 714: 136745

Mellahi D, Zerdoumi R, Rebbani N, Gheid A (2015). The relationship between chlorine consumption and trihalomethane formation from hydrophobic and transphilic fractions: A comparative study between two dams of east Algeria. Journal of Water Reuse and Desalination, 5 (1): 72–82

Oliver B G, Carey J H (1977). Photochemical Production of Chlorinated Organics in Aqueous Solutions Containing Chlorine. Environmental Science & Technology, 11(9): 893–895

Pan Y, Zhang X R, Zhai J P (2015). Whole pictures of halogenated disinfection byproducts in tap water from China's cities. Frontiers of Environmental Science & Engineering, 9(1): 121–130

Qian Y, Wang W, Boyd J M, Wu M, Hrudey S E, Li X F (2013). UV-induced transformation of four halobenzoquinones in drinking water. Environmental Science & Technology, 47(9): 4426–4433

Qin F, Zhao Y Y, Zhao Y, Boyd J M, Zhou W, Li X F (2010). A toxic disinfection by-product, 2,6-dichloro-1,4-benzoquinone, identified in

drinking water. Angewandte Chemie (International ed. in English), 49(4): 790–792

Richardson S D, Ternes T A (2014). Water analysis: Emerging contaminants and current issues. Analytical Chemistry, 86(6): 2813–2848

Saha A, Kawade M N, Upadhyaya H P, Kumar A, Naik P D (2013). Photoexcitation of 2-bromo-2-chloro-1,1,1-trifluoroethane (halothane) to repulsive surface nσ*(C–Br) at 234 nm: Dynamics of C–Br and C–Cl bond rupture. Chemical Physics, 416: 1–10

Sharma V K, Yang X, Cizmas L, Mcdonald T J, Luque R, Sayes C M, Yuan B L, Dionysiou D D (2017). Impact of metal ions, metal oxides, and nanoparticles on the formation of disinfection byproducts during chlorination. Chemical Engineering Journal, 317: 777–792

Sharma V K, Yu X, McDonald T J, Jinadatha C, Dionysiou D D, Feng M (2019). Elimination of antibiotic resistance genes and control of horizontal transfer risk by UV-based treatment of drinking water: A mini review. Frontiers of Environmental Science & Engineering, 13(3): 37

Shu Z, Li C, Belosevic M, Bolton J R, El-Din M G (2014). Application of a solar UV/chlorine advanced oxidation process to oil sands process-affected water remediation. Environmental Science & Technology, 48(16): 9692–9701

Smith M B (2017). Organic Synthesis (4th Edition). Smith M B, ed. Boston: Academic Press, 97–160

Sun P, Lee W N, Zhang R, Huang C H (2016). Degradation of DEET and Caffeine under UV/Chlorine and Simulated Sunlight/Chlorine Conditions. Environmental Science & Technology, 50(24): 13265–13273

Wang W, Moe B, Li J H, Qian Y C, Zheng Q, Li X F (2016). Analytical characterization, occurrence, transformation, and removal of the emerging disinfection byproducts halobenzoquinones in water. Trends in Analytical Chemistry, 85: 97–110

Wang W, Qian Y, Boyd J M, Wu M, Hrudey S E, Li X F (2013a). Halobenzoquinones in swimming pool waters and their formation from personal care products. Environmental Science & Technology, 47(7): 3275–3282

Wang W, Qian Y, Boyd J M, Wu M, Hrudey S E, Li X F (2013b). Halobenzoquinones in swimming pool waters and their formation from personal care products. Environmental Science & Technology, 47(7): 3275–3282

Wang W, Qian Y, Li J, Moe B, Huang R, Zhang H, Hrudey S E, Li X F (2014). Analytical and toxicity characterization of halo-hydroxyl-benzoquinones as stable halobenzoquinone disinfection byproducts in treated water. Analytical Chemistry, 86(10): 4982–4988

Wang H, Ma D, Shi W, Yang Z, Cai Y, Gao B (2021). Formation of disinfection by-products during sodium hypochlorite cleaning of fouled membranes from membrane bioreactors. Frontiers of Environmental Science & Engineering, 15(5): 102

Westerhoff P, Chao P, Mash H (2004). Reactivity of natural organic matter with aqueous chlorine and bromine. Water Research, 38(6): 1502–1513

Wu Q Y, Yan Y J, Lu Y, Du Y, Liang Z F, Hu H Y (2020). Identification of important precursors and theoretical toxicity evaluation of byproducts driving cytotoxicity and genotoxicity in chlorination. Frontiers of Environmental Science & Engineering, 14(2): 25

Yang C, Sun W, Ao X (2020). Bacterial inactivation, DNA damage, and faster ATP degradation induced by ultraviolet disinfection. Frontiers of Environmental Science & Engineering, 14(1): 13

Yang P, Kong D, Ji Y, Lu J, Yin X, Zhou Q (2018). Chlorination and chloramination of benzophenone-3 and benzophenone-4 UV filters. Ecotoxicology and Environmental Safety, 163: 528–535

Young T R, Li W, Guo A, Korshin G V, Dodd M C (2018). Characterization of disinfection byproduct formation and associated changes to dissolved organic matter during solar photolysis of free available chlorine. Water Research, 146: 318–327

Zhang K, Parker K M (2018). Halogen Radical Oxidants in Natural and Engineered Aquatic Systems. Environmental Science & Technology, 52(17): 9579–9594

Zhang X, Wei D, Sun X, Bai C, Du Y (2021). Free available chlorine initiated Baeyer-Villiger oxidation: A key mechanism for chloroform formation during aqueous chlorination of benzophenone UV filters. Environmental Pollution, 268(Pt A): 115737

Zhang Y S, Shao Y S, Gao N Y, Gao Y Q, Chu W H, Li S, Wang Y, Xu S X (2018). Kinetics and by-products formation of chloramphenicol (CAP) using chlorination and photocatalytic oxidation. Chemical Engineering Journal, 333: 85–91

Zhao Q, Shang C, Zhang X, Ding G, Yang X (2011). Formation of halogenated organic byproducts during medium-pressure UV and chlorine coexposure of model compounds, NOM and bromide. Water Research, 45(19): 6545–6554

Zhao Y, Anichina J, Lu X, Bull R J, Krasner S W, Hrudey S E, Li X F (2012). Occurrence and formation of chloro- and bromo-benzoquinones during drinking water disinfection. Water Research, 46(14): 4351–4360

Zhao Y, Qin F, Boyd J M, Anichina J, Li X F (2010). Characterization and determination of chloro- and bromo-benzoquinones as new chlorination disinfection byproducts in drinking water. Analytical Chemistry, 82(11): 4599–4605

Zhong C, Zhao H, Han Q, Cao H, Duan F, Shen J, Xie Y, Guo W, Sun S (2020). Coupling-oxidation process promoted ring-opening degradation of 2-mecapto-5-methyl-1,3,4-thiadizaole in wastewater. Water Research, 186: 116362

Zhu Q, Gu A, Li D, Zhang T, Xiang L, He M (2021). Online recognition of drainage type based on UV-vis spectra and derivative neural network algorithm. Frontiers of Environmental Science & Engineering, 15(6): 136